

Enhancing Autler-Townes splittings by ultrafast XUV pulses

Wei-Chao Jiang^{1,*}, Hao Liang², Shun Wang,¹ Liang-You Peng^{2,3,4,†} and Joachim Burgdörfer⁵

¹College of Physics and Optoelectronic Engineering, Shenzhen University, Shenzhen 518060, China

²State Key Laboratory for Mesoscopic Physics and Frontiers Science Center for Nano-optoelectronics, School of Physics, Peking University, 100871 Beijing, China

³Collaborative Innovation Center of Quantum Matter, Beijing 100871, China

⁴Collaborative Innovation Center of Extreme Optics, Shanxi University, Taiyuan 030006, China

⁵Institute for Theoretical Physics, Vienna University of Technology, Wiedner Hauptstraße 8-10, A-1040 Vienna, Austria, EU



(Received 15 May 2021; accepted 16 July 2021; published 25 August 2021)

We study the photoelectron spectra of hydrogen and helium ionized by intense ultrafast two-color XUV laser pulses by numerically solving the time-dependent Schrödinger equation. The photon energy of the pump pulse is tuned to the $1s$ - $2p$ excitation energy, inducing Rabi oscillations between these bound states and forming an Autler-Townes (AT) doublet of dressed states. When ionized by a time-delayed ultrafast XUV pulse with duration shorter than the Rabi oscillation period, we find novel and drastically enhanced AT splittings in the photoionization spectrum. We identify their origin in terms of the temporal interference of two attosecond wave packets whose spectral distribution is controlled by the interplay between Rabi frequency and bandwidth of the probe pulse. These time-dependent features in the spectra can be much larger than the standard AT spacing induced by the pump pulse alone and can be controlled by the time delay and the duration of the probe pulse.

DOI: [10.1103/PhysRevResearch.3.L032052](https://doi.org/10.1103/PhysRevResearch.3.L032052)

One of the most prominent features of strong coupling between the radiation field and matter are Rabi oscillations [1–7]. Irradiating a material system with intense radiation at the resonance frequency between two of its bound states allows for an efficient and reversible transfer of population [8–10]. Rabi oscillations have been identified in a large variety of physical systems including ultracold atoms [11,12], Rydberg atoms [13], molecules [14–16], metal nanostructures [17], Josephson-junction circuits [18], and quantum dots [19] and for a wide range of frequencies from radio frequencies to the ultraviolet. Recently, Rabi oscillations have also been observed in the extreme ultraviolet (XUV) regime [20,21], enabled by the development of the coherent high-intensity XUV pulse sources [22–25]. The real-time observation of the Rabi oscillations has been realized by detecting the resonance fluorescence [14,19], the state-dependent index of refraction [26], the birefringence [27], the differential reflectivity spectra [17], and the photoelectron spectra [28,29]. Rabi oscillations of the populations of two bound states are closely connected to the formation of a doublet of “dressed” quasienergy states separated by an energy spacing given by the Rabi frequency Ω_R , $\Delta E = \hbar\Omega_R$. Spectral features of such doublets are referred to as Autler-Townes (AT) splittings [30]. One important appli-

cation of the AT splittings is the electromagnetically induced transparency (EIT), which has been utilized to laser cooling the long strings of atoms [31] and to slow light [32]. EIT in the XUV regime has been realized by multicolor, multiphoton XUV+IR ionization of helium [33]. AT splittings have been identified in a large variety of settings [34–42] including in multiphoton ionization [40–42], in double ionization [43,44], and even in the absence of population oscillation of the initial ground state when an ionic core transition is resonantly driven [45,46].

Conventional AT splittings appear for multicycle driving fields with (near) constant amplitude and duration long compared to the Rabi period $T_R = 2\pi/\Omega_R$, and are well described by Floquet theory [47]. Here we explore a novel regime of time-resolved Rabi oscillations resulting in time-dependent energy spacings accessible by ultrashort XUV pulses. We consider an intense (10^{14} W/cm²) pump pulse resonantly tuned to transition from the ground state to an excited state (in the following numerical examples to the $1s$ - $2p$ transitions of hydrogen and helium) giving rise to Rabi oscillations of coherent population transfer. We probe the time-resolved population dynamics by an ionizing ultrashort XUV probe pulse whose duration is shorter than the Rabi period T_R . Remarkably, the resulting time-resolved ionization spectrum features time-delay dependent AT splittings that can considerably exceed their steady-state counterpart. We identify the origin of these spectral features observed in our numerical solutions of the time-dependent Schrödinger equation (TDSE) in terms of temporal interferences between two attosecond wave packets which leave a pronounced time-delay dependent mark on the spectrum. We present a simple analytical model for these dynamical AT splittings which quantitatively predicts the en-

*jiang.wei.chao@szu.edu.cn

†liangyou.peng@pku.edu.cn

hanced energy spacing as a function of the Rabi frequency Ω_R and the spectral width $\Delta\omega$ of the ultrashort XUV pulse.

The linearly polarized vector potential of either the pump ($i = 1$) or the probe pulse ($i = 2$) is expressed as $A_i(t) = A_{0,i}f_i(t)\sin(\omega_i t)$, where $A_{0,i}$ is the amplitude, ω_i is the frequency, and $f_i(t)$ is the normalized envelope of the pulse. The electric field follows from $F_i(t) = -dA_i(t)/dt$. The pump pulse is chosen to be resonant with the $1s$ - $2p$ transition in atomic units $\omega_1 = E_{2p} - E_{1s}$ ($= 0.375$ a.u. for hydrogen), its effective duration controlled by $f_1(t)$ to be long compared to the Rabi period T_R . The frequency of the probe pulse ($\omega_2 = 1.3$ a.u.) is chosen to enable direct photoionization of the ground state to a region of the continuum spectrum well separated from above-threshold ionization peaks induced by the pump pulse. The pump pulse generates oscillations with frequency [41]

$$\Omega_R(t) = F_{0,1}f_1(t)\langle 2p|z|1s \rangle, \quad (1)$$

where $F_{0,1}$ is the peak amplitude of the electric field of the pump pulse, and $\langle 2p|z|1s \rangle = \frac{256}{243\sqrt{2}}$ for hydrogen. For the pump laser pulse with peak intensity 10^{14} W/cm², the maximum Rabi frequency Ω_R at the peak of the envelope is estimated to be 0.04 a.u., corresponding to $T_R = 3.8$ fs. The pump pulse alone can ionize the hydrogen atom by absorbing one photon in the dressed $2p$ state or by (at least) two photons in the dressed $1s$ state [Fig. 1(a), left inset]. The pump pulse thus not only drives coherent population transfer but also induces damping and decoherence into the Rabi flopping. At the present pump intensities, the two-photon ionization path from the $1s$ state is negligible compared to the one-photon path from the $2p$ state [48]. The one-photon ionization spectrum caused by the long pump pulse from the field dressed $2p$ state near $E = 0.25$ a.u. maps out the standard AT splitting with $\Delta E_{AT} = 0.029$ a.u., which is slightly smaller than Ω_R , as expected for the envelope f_1 . The replica of the peak-split spectrum with $\Delta E_{AT} = 0.03$ a.u. can be observed near the two-photon ATI peak from $2p$ state near $E = 0.625$ a.u.

Novel spectral features appear when the Rabi oscillations are probed by a time-delayed ultrafast nonresonant XUV pulse with time delay τ whose duration is short compared to the Rabi period T_R thereby mapping out their temporal dynamics. The probe pulse transfers the population of the ground state to the continuum by one-photon absorption, producing photoelectrons at energy around $E = 0.8$ a.u. [Fig. 1(a)] with the spectrum displaying a pronounced dependence on τ . In Fig. 1 we have used a \cos^2 envelope of the probe pulse $f_2(t) = \cos^2(\omega_2 t/2N)$ with the number of cycles N varying between 15 and 40 corresponding to effective pulse durations between $T_2 = 630$ as and 1.7 fs. Horizontal cuts through the ionization spectra at $E = 0.8$ a.u. [Fig. 1(a)], accordingly, map out the oscillating occupations of the $1s$ level directly extracted from the TDSE [Fig. 1(b)]. For the present pump pulse, the population of the ground state oscillates for about two Rabi cycles with zero population at two points in time around $t = -95$ and 74.8 a.u. and with peak population at around $t = -10.4$ a.u. For all three probe pulse durations tested, the photoelectron spectra accurately reproduce the times where the population reaches its minima and maxima. As expected, the Rabi oscillations extracted from the shortest probe pulse

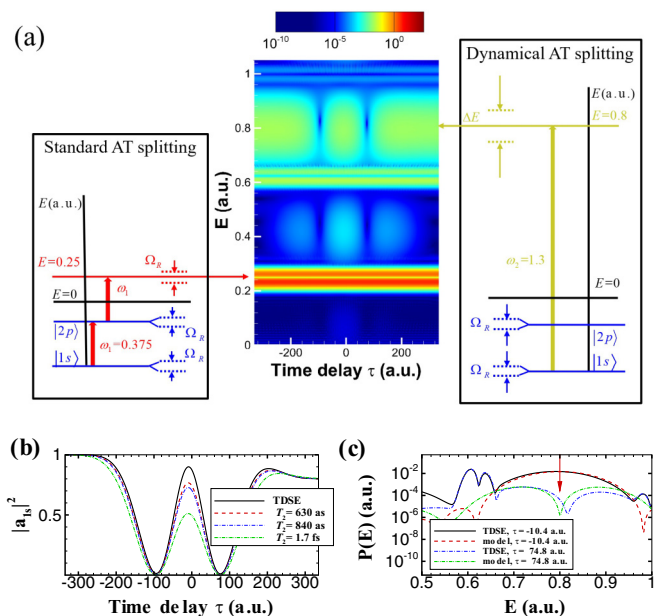


FIG. 1. (a) The delay-dependent photoelectron energy spectra of hydrogen atom from numerical TDSE calculations. The pump pulse has peak intensity of 0.1 PW/cm² and duration of $T_1 = 5.9$ fs. The intensity of the ultrashort ($T_2 = 630$ as) probe pulse is 0.05 PW/cm². Left inset: Standard Autler-Townes (AT) splittings are observed near $E = 0.25$ a.u. reached by one-photon ionization of the excited $2p$ state, or by two-photon ionization of the ground state, by ω_1 photons from the pump field. The spectrum near $E = 0.25$ a.u. is independent of the delay time τ . Right inset: Observation of the dynamical AT splitting by absorption of an ω_2 photon from the probe field. The spectrum features strong variation with τ . (b) The Rabi oscillation of the ground state extracted from the TDSE calculation by projecting the wave function to the ground state compared with the delay-dependent photoelectron signal at $E = 0.8$ a.u., as observed by horizontal cut through (a). (c) Time-resolved spectra [vertical cuts through (a)] for two different delay times $\tau = -10.4$ a.u. and $\tau = 74.8$ a.u. displaying a pronounced AT splitting near $E = 0.8$ a.u.

is the closest to the full TDSE results. The damping of the amplitude of the Rabi oscillation originates from the strong coupling from the bound states to the continuum by the pump pulse.

Unexpected new spectral features appear as a function of the time delay between pump and probe [Fig. 1(c)], displaying a pronounced splitting of the photoionization peak near $E = 0.8$ a.u., identified in the following as dynamically enhanced Autler-Townes splittings. A single peak near $E = 0.8$ a.u. appears when the probe pulse is located around the peak ($\tau = -10.4$ a.u.) of the ground-state population. This peak is, however, split into a doublet when the probe pulse is located at the time of the minima in the population ($\tau = 74.8$ a.u.). The size of the splitting ΔE is strongly dependent on the delay τ and can considerably exceed the expected steady-state AT splitting (Fig. 2). It is most pronounced for the shortest probe pulses employed ($T_2 = 630$ as) but still clearly visible for somewhat longer pulses ($T_2 = 1.7$ fs) as the probe pulse duration is still shorter than the Rabi period T_R .

To uncover the origin of the dynamical enhancement of the AT splitting, we have developed a simplified semianalytical

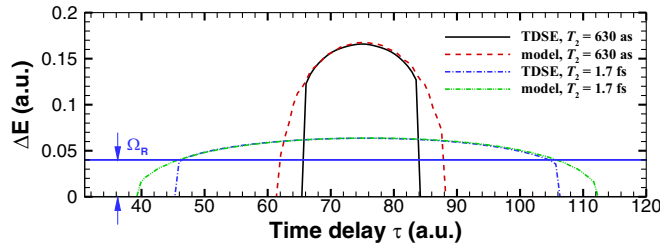


FIG. 2. The spacing ΔE of the dynamical AT splitting as a function of the time delay τ . The blue horizontal line marks the maximum Rabi frequency $\Omega_R = 0.04$ a.u. indicating the size of the standard AT splitting. The TDSE results are compared with the model results (see the text). The parameters of the pump pulse are the same as in Fig. 1. The probe pulse has peak intensity of 0.05 PW/cm², and duration of $T_2 = 630$ as or 1.7 fs.

model. Our starting point is the expression for the energy-differential and delay-time dependent ionization probability in first-order perturbation theory in the weak probe field [49–52]

$$P(E; \tau) = \left| \int dt d(E) a_{1s}(t) A_2(t - \tau) e^{i\omega_{Ei}t} \right|^2, \quad (2)$$

where the temporal center of the probe pulse is located at $t = \tau$, $d(E) = \langle \Psi_E | \frac{\partial}{\partial z} | \Psi_{1s} \rangle$ is the dipole matrix element between the ground state Ψ_{1s} and the continuum state Ψ_E , and $\omega_{Ei} = E + I_p$ is the energy separation between the two states with ionization potential $I_p = 0.5$ a.u. The nonperturbative influence of the pump pulse is included by the time-dependent amplitude $a_{1s}(t)$ of the ground state displaying Rabi oscillations. For probe pulses very short compared to T_R , $T_2 \ll T_R$, Eq. (2) can be simplified to

$$P(E; \tau) = |a_{1s}(\tau)|^2 \left| \int dt d(E) A_2(t) e^{i\omega_{Ei}t} \right|^2, \quad (3)$$

indicating that the delay-time variation of the ionization probability directly mirrors the oscillation of the ground state occupation $|a_{1s}(\tau)|^2$. Equation (3) provides an intuitive explanation for the close agreement between the energy-differential ionization probability at $E = 0.8$ a.u. and the TDSE solution for $|a_{1s}(\tau)|^2$ [Fig. 1(b)].

For a monochromatic pump pulse $A_1(t) = A_{0,1}(t) \cos(\omega_1 t)$, the evolution of the amplitude of the ground state is in two-level approximation [53]

$$a_{1s}(t) = \cos(\Omega_R t / 2), \quad (4)$$

for which the pump pulse is assumed to be turned on at $t = 0$. The amplitude $a_{1s}(t)$ changes the sign, i.e., the $a_{1s}(t)$ will go through a phase jump of π at the time of the zero crossing of the population. This phase jump leads to a destructive interference in the ionization amplitude and the suppression of ionization probability even if the ultrashort limit $T_2 \ll T_R$ is not yet reached [Fig. 3(a)]. This temporal path interference is key to the dynamical AT splitting ΔE observed by an ultrashort pulse with spectral width $\Delta\omega \propto 1/T_2$ [Fig. 3(b)].

According to Eq. (2), the photoelectron spectrum resulting from the transition at τ directly mimics the square of the Fourier transform of the time dependent signal

$$\tilde{A}(t; \tau) = a_{1s}(t) A_2(t - \tau). \quad (5)$$

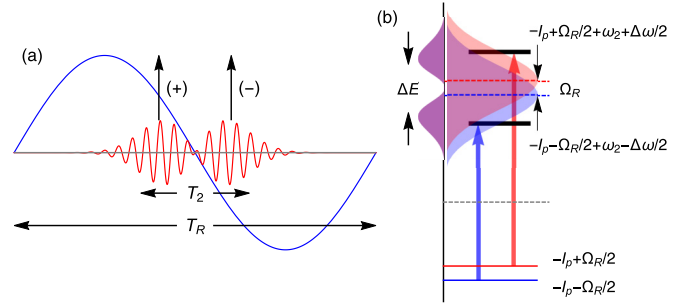


FIG. 3. Time domain (a) and spectral domain (b) view of the ionization path interference resulting in dynamically enhanced AT splitting.

When the probe pulse is temporally localized near the zero point of $a_{1s}(t)$, the signal $\tilde{A}(t; \tau)$ in Eq. (5) contains two time-delayed pulses with opposite signs [Fig. 3(a)] and, thus, generates two ionization bursts phase shifted relative to one another by π . The Fourier spectrum of the signal $\tilde{A}(t; \tau)$, $\mathcal{F}(\omega; \tau) = C \left| \int dt \tilde{A}(t; \tau) e^{i(\omega + I_p)t} \right|^2$ shown in Figs. 1(c) and 2 perfectly reproduces the large separation, delay dependence, and pulse-duration dependence of the dynamical AT splitting observed in TDSE calculations. The delay dependence and the pulse-width dependence of the AT splitting can be easily understood in terms of this temporal interference: only when the ultrashort probe pulse is near the zero point of the population, the ionization is split into two time-delayed electron emission bursts. Indeed, the width of the temporal window in Fig. 2 is a fraction of the pulse width ($\sim 0.8T_2$).

For an analytical estimate of the spectral separation of the two AT peaks, we approximate the ground-state amplitude by Eq. (4) and express the photoionization probability in terms of the coherent superposition of the two time-delayed electron wave packets,

$$P(E; \tau) = \frac{1}{4} |d(E)|^2 \times \left| \mathbb{F}(\omega_{Ei} + \Omega_R/2) + e^{-i\Omega_R \tau} \mathbb{F}(\omega_{Ei} - \Omega_R/2) \right|^2, \quad (6)$$

where $\mathbb{F}(\omega)$ is the Fourier transform of the probe laser pulse defined as $\mathbb{F}(\omega) = \int_{-\infty}^{\infty} dt A_2(t) e^{i\omega t}$. The two terms in Eq. (6) can be understood as the electron wave packets emitted from photon-dressed $1s$ states with energies $E = -I_p - \Omega_R/2$ and $E = -I_p + \Omega_R/2$, respectively [Fig. 3(b)]. The peak positions of the two terms taken separately are located at $E = \omega_2 - I_p - \Omega_R/2$ and $E = \omega_2 - I_p + \Omega_R/2$, respectively. However, the coherent superposition Eq. (6) leads to a peak shift controlled by the delay τ and the spectral width $\Delta\omega$ of the probe pulse. At the Rabi phase $\Omega_R \tau = \pi$ where the population of $1s$ state is zero, the interference of the two terms is completely destructive at energy $E = 0.8$ a.u. and the peak position is determined by the difference $\mathbb{F}(\omega_{Ei} + \Omega_R/2) - \mathbb{F}(\omega_{Ei} - \Omega_R/2)$. Assuming for simplicity a Gaussian pulse with envelope $f_2(t) = \exp(-2 \ln 2 \frac{t^2}{T_2^2})$, $\mathbb{F}(\omega)$ is explicitly given by

$$\mathbb{F}(\omega) = \frac{A_{0,2}}{\Delta\omega} \sqrt{\frac{8\pi}{\ln(2)}} \exp \left[-2 \ln(2) \frac{(\omega - \omega_2)^2}{\Delta\omega^2} \right], \quad (7)$$

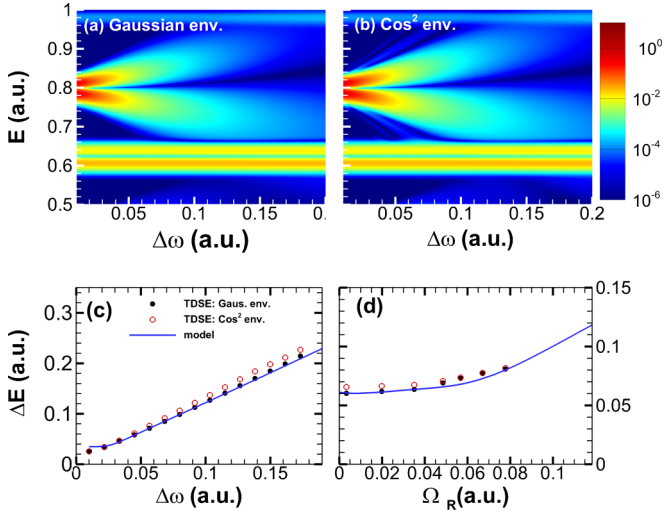


FIG. 4. (a) and (b) The photoelectron spectra as a function of the spectral width $\Delta\omega$ of the probe pulse for two different envelopes. The pump pulse is the same as in Fig. 1, the intensity of the probe pulse is 5×10^{13} W/cm², and the time delay τ is 74.8 a.u. The effective energy spacing ΔE of the split peak extracted from (a) and (b) are plotted as a function of $\Delta\omega$ at fixed $\Omega_R = 0.35$ a.u. in (c) and as a function of Ω_R at fixed spectral width $\Delta\omega = 0.05$ a.u. of the probe pulse in (d). In the TDSE calculations of (d), the Rabi frequency Ω_R is varied by varying the intensity of the pump pulse, and the probe pulse with intensity 1×10^{15} W/cm² is always temporally located at the zero crossing of the population of the initial $1s$ state.

where the spectral width $\Delta\omega$ is related to the pulse width T_2 by $\Delta\omega = 4 \ln 2/T_2$.

Using Eq. (7) we find after some algebraic manipulations for the dynamical AT splitting

$$\Delta E = \Omega_R + 2|\delta E(\gamma)|, \quad (8)$$

with δE the solution of a transcendental equation which can be approximated in first iteration by

$$\delta E(\gamma) = -\Delta\omega \frac{[1 + \ln(2)]\gamma + 2 \ln(2)\gamma^2}{4\gamma + \gamma^2 + 2 \ln(2)\gamma + 4 \ln(2)\gamma^2 - 1}. \quad (9)$$

The dynamical splitting is increased compared to the Rabi splitting Ω_R linearly with $\Delta\omega$ and is a function of the dimensionless ratio of Rabi frequency to spectral width of the ultrashort probe pulse $\gamma = \Omega_R/\Delta\omega$. As expected, in the limit $\Delta\omega \rightarrow 0$, the enhanced AT splitting is reduced to the standard AT splitting [Eq. (8)]. The analytical model reproduces the results of the full numerical TDSE calculations remarkably well [Figs. 4(c) and 4(d)]. We give in Fig. 4 results for both a Gaussian and a \cos^2 envelope. The shape of the envelope has only a minor influence, as expected. The separation ΔE displays an asymptotically linear dependence on the spectral width $\Delta\omega$ [Fig. 4(c)]. Indeed, in the limit $\gamma \rightarrow 0$ δE [Eq. (8)] is $-(1 + \ln 2)/4 \ln 2 \Delta\omega \approx -0.6\Delta\omega$, resulting in the asymptotic solution

$$\Delta E = 1.2\Delta\omega \quad (10)$$

for $\gamma \rightarrow 0$. Thus, with increasing $\Delta\omega$, the dynamically induced excitation gap in the ionization spectrum becomes increasingly prominent.

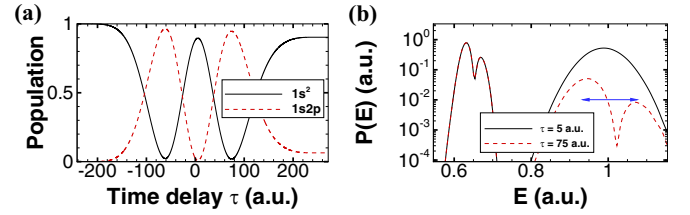


FIG. 5. Dynamical AT splitting in single ionization of He observed in full two-electron TDSE calculations. (a) The Rabi oscillations of the ground state ($1s^2$) and the first excited state ($1s2p$) induced by the pump pulse. (b) The single-ionization energy spectrum shown for two time delays of the probe pulse ($\omega_2 = 1.9037$ a.u.). The length of the blue arrow indicates the prediction [Eq. (10)] for splitting $\Delta E = 1.2\Delta\omega = 0.12$ a.u.

To demonstrate the generality of the present dynamical AT splitting, we have performed much more challenging numerical calculations for the full-dimensional TDSE of the two-electron helium. The pump pulse with intensity 5×10^{14} W/cm² and photon energy 21.22 eV is used to excite the Rabi oscillations between the ground state $1s^2$ and the first excited state $1s2p$ [Fig. 5(a)]. A time-delayed probe pulse with the same intensity, the photon energy $\omega_2 = 1.9037$ a.u., and the spectral width $\Delta\omega = 0.1$ a.u. transfers the $1s^2$ state to a continuum state with a kinetic energy around $E = 1$ a.u. When the probe pulse is located in time around $\tau = 5$ a.u. corresponding to the maximum population of state $1s^2$, the single-ionization spectrum shows a prominent single peak at $E = 1$ a.u. This single peak is split into a doublet as the time delay is changed to the time $\tau = 75$ a.u. corresponding to the minimal population of state $1s^2$ [Fig. 5(b)]. The separation of the dynamical AT splitting agrees well with the asymptotic solution Eq. (10), further supporting our analytical model.

In summary, we have demonstrated a dynamically enhanced Aulter-Townes (AT) type splitting in the photoemission spectrum of atoms in a two-color XUV-pump and XUV-probe protocol. The experimental verification of the present dynamical AT splitting may become in reach as an intense (X)UV pulse is only required for the lower frequency pump pulse while only a weak attosecond probe pulse is involved in the one-photon ionization. We find that the separation of the dynamical AT splitting can be much larger than the Rabi frequency and be controlled by the duration and the time delay of the probe pulse. The ultrashort duration of the probe pulse in comparison with the Rabi period is essential to observe the dynamical AT splitting. We have derived an analytical estimate for the separation of the dynamical AT splitting, which depends on both the Rabi frequency and the spectral width of the probe pulse. The present protocol explicitly demonstrated here for one-electron and two-electron atoms can be generalized and applied to a large variety of physical systems provided that the bound-state population can be efficiently and coherently modulated. Extensions to other frequencies and to multiple ionization are straightforward. It opens up new avenues for temporal control of the photoemission spectra by ultrashort (sub)femtosecond pulses. The spacing of the dynamical AT splittings may be used

to calibrate the effective temporal length of the, possibly chirped, ultrashort pulse. Conceptually most interestingly, photoemission lines at their nominal energetic positions can be “bleached,” i.e., switched to a “dark” state by a suitable combination of time delay and spectral width of the ionizing pulse. This can be viewed as a dynamical version of the EIT window. The underlying mechanism is, however, different. While the dark state in the EIT results from the destructive interference between the direct path to the final state and the indirect path involving a third state [54] resembling a Fano “window” resonance [55], in the present scenario it results in the time domain from the destructive interference of two attosecond wave packets launched temporally delayed relative to another. Thus, the dynamical AT splitting

provides a prototypical example for the manipulation of spectral features, conventionally viewed as time independent, by (sub)femtosecond electromagnetic pulses.

W.-C.J. acknowledges the inspiring discussions with Prof. Y. Zhou and Prof. M. Li. This work is supported by the National Natural Science Foundation of China (NSFC) (Grants No. 12074265, No. 11804233, No. 11747013, No. 11961131008, and No. 11725416), by the National Key R&D Program of China (Grant No. 2018YFA0306302), and by Grants No. FWF-SFB041-VICOM (Austria), No. FWF-SFB049-NEXTLITE (Austria), No. FWF-W1243-SOLIDS4FUN (Austria) and COST ACTION CA18234 (ECST).

-
- [1] I. I. Rabi, On the process of space quantization, *Phys. Rev.* **49**, 324 (1936).
- [2] P. Knight and P. Milonni, The Rabi frequency in optical spectra, *Phys. Rep.* **66**, 21 (1980).
- [3] B. R. Mollow, Power spectrum of light scattered by two-level systems, *Phys. Rev.* **188**, 1969 (1969).
- [4] M. Ruggenthaler and D. Bauer, Rabi Oscillations and Few-Level Approximations in Time-Dependent Density Functional Theory, *Phys. Rev. Lett.* **102**, 233001 (2009).
- [5] K. Nasiri Avanaki, D. A. Telnov, and S.-I. Chu, Harmonic generation of Li atoms in one- and two-photon Rabi-flopping regimes, *Phys. Rev. A* **94**, 053410 (2016).
- [6] V. Stooß, S. M. Cavaletto, S. Donsa, A. Blättermann, P. Birk, C. H. Keitel, I. Březinová, J. Burgdörfer, C. Ott, and T. Pfeifer, Real-Time Reconstruction of the Strong-Field-Driven Dipole Response, *Phys. Rev. Lett.* **121**, 173005 (2018).
- [7] A. F. Linskens, I. Holleman, N. Dam, and J. Reuss, Two-photon Rabi oscillations, *Phys. Rev. A* **54**, 4854 (1996).
- [8] K. Bergmann, H. Theuer, and B. W. Shore, Coherent population transfer among quantum states of atoms and molecules, *Rev. Mod. Phys.* **70**, 1003 (1998).
- [9] C. Trallero-Herrero, J. L. Cohen, and T. Weinacht, Strong-Field Atomic Phase Matching, *Phys. Rev. Lett.* **96**, 063603 (2006).
- [10] R. G. Unanyan, B. W. Shore, and K. Bergmann, Laser-driven population transfer in four-level atoms: Consequences of non-Abelian geometrical adiabatic phase factors, *Phys. Rev. A* **59**, 2910 (1999).
- [11] M. Reetz-Lamour, J. Deiglmayr, T. Amthor, and M. Weidemüller, Rabi oscillations between ground and Rydberg states and van der Waals blockade in a mesoscopic frozen Rydberg gas, *New J. Phys.* **10**, 045026 (2008).
- [12] X. Chen and J. A. Yeazell, Observation of a Nondecaying Wave Packet in a Two-Electron Atom, *Phys. Rev. Lett.* **81**, 5772 (1998).
- [13] B. Huber, T. Baluktian, M. Schlagmüller, A. Kölle, H. Kübler, R. Löw, and T. Pfau, GHz Rabi Flopping to Rydberg States in Hot Atomic Vapor Cells, *Phys. Rev. Lett.* **107**, 243001 (2011).
- [14] M. Rezai, J. Wrachtrup, and I. Gerhardt, Detuning dependent Rabi oscillations of a single molecule, *New J. Phys.* **21**, 045005 (2019).
- [15] A. Palacios, H. Bachau, and F. Martín, Step-ladder Rabi oscillations in molecules exposed to intense ultrashort VUV pulses, *Phys. Rev. A* **74**, 031402(R) (2006).
- [16] A. Palacios, H. Bachau, and F. Martín, Excitation and ionization of molecular hydrogen by ultrashort VUV laser pulses, *Phys. Rev. A* **75**, 013408 (2007).
- [17] P. Vasa, W. Wang, R. Pomraenke, M. Lammers, M. Maiuri, C. Manzoni, G. Cerullo, and C. Lienau, Real-time observation of ultrafast Rabi oscillations between excitons and plasmons in metal nanostructures with j-aggregates, *Nat. Photon.* **7**, 128 (2013).
- [18] Y. Nakamura, Y. A. Pashkin, and J. S. Tsai, Rabi Oscillations in a Josephson-Junction Charge Two-Level System, *Phys. Rev. Lett.* **87**, 246601 (2001).
- [19] A. Müller, E. B. Flagge, P. Bianucci, X. Y. Wang, D. G. Deppe, W. Ma, J. Zhang, G. J. Salamo, M. Xiao, and C. K. Shih, Resonance Fluorescence from a Coherently Driven Semiconductor Quantum Dot in a Cavity, *Phys. Rev. Lett.* **99**, 187402 (2007).
- [20] M. Fushitani, C. N. Liu, A. Matsuda, T. Endo, Y. Toida, M. Nagasono, T. Togashi, M. Yabashi, T. Ishikawa, Y. Hikosaka, T. Morishita, and A. Hishikawa, Femtosecond two-photon Rabi oscillations in excited He driven by ultrashort intense laser fields, *Nat. Photon.* **10**, 102 (2016).
- [21] T. Sako, J. Adachi, A. Yagishita, M. Yabashi, T. Tanaka, M. Nagasono, and T. Ishikawa, Suppression of ionization probability due to Rabi oscillations in the resonance two-photon ionization of He by EUV free-electron lasers, *Phys. Rev. A* **84**, 053419 (2011).
- [22] T. Wittmann, B. Horvath, W. Helml, M. G. Schaetzel, X. Gu, A. L. Cavalieri, G. G. Paulus, and R. Kienberger, Single-shot carrier-envelope phase measurement of few-cycle laser pulses, *Nat. Phys.* **5**, 357 (2009).
- [23] D. Gauthier, P. c. v. R. Ribič, G. De Ninno, E. Allaria, P. Cinquegrana, M. B. Danailov, A. Demidovich, E. Ferrari, L. Giannessi, B. Mahieu, and G. Penco, Spectrotemporal Shaping of Seeded Free-Electron Laser Pulses, *Phys. Rev. Lett.* **115**, 114801 (2015).
- [24] E. P. Kanter, B. Krässig, Y. Li, A. M. March, P. Ho, N. Rohringer, R. Santra, S. H. Southworth, L. F. DiMauro, G. Doumy, C. A. Roedig, N. Berrah, L. Fang, M. Hoener, P. H. Bucksbaum, S. Ghimire, D. A. Reis, J. D. Bozek, C. Bostedt,

- M. Messerschmidt *et al.*, Unveiling and Driving Hidden Resonances with High-Fluence, High-Intensity X-Ray Pulses, *Phys. Rev. Lett.* **107**, 233001 (2011).
- [25] Y. Zhang, T.-M. Yan, and Y. H. Jiang, Ultrafast Mapping of Coherent Dynamics and Density Matrix Reconstruction in a Terahertz-Assisted Laser Field, *Phys. Rev. Lett.* **121**, 113201 (2018).
- [26] P. J. Windpassinger, D. Oblak, P. G. Petrov, M. Kubasik, M. Saffman, C. L. Garrido Alzar, J. Appel, J. H. Müller, N. Kjærgaard, and E. S. Polzik, Nondestructive Probing of Rabi Oscillations on the Cesium Clock Transition near the Standard Quantum Limit, *Phys. Rev. Lett.* **100**, 103601 (2008).
- [27] S. Chaudhury, G. A. Smith, K. Schulz, and P. S. Jessen, Continuous Nondemolition Measurement of the Cs Clock Transition Pseudospin, *Phys. Rev. Lett.* **96**, 043001 (2006).
- [28] M. Flögel, J. Durá, B. Schütte, M. Ivanov, A. Rouzée, and M. J. J. Vrakking, Rabi oscillations in extreme ultraviolet ionization of atomic argon, *Phys. Rev. A* **95**, 021401(R) (2017).
- [29] X. Chen, W. Cao, Z. Li, Z. Yang, Q. Zhang, and P. Lu, Probing laser-driven bound-state dynamics using attosecond streaking spectroscopy, *Phys. Rev. A* **102**, 053119 (2020).
- [30] S. H. Autler and C. H. Townes, Stark effect in rapidly varying fields, *Phys. Rev.* **100**, 703 (1955).
- [31] R. Lechner, C. Maier, C. Hempel, P. Jurcevic, B. P. Lanyon, T. Monz, M. Brownnutt, R. Blatt, and C. F. Roos, Electromagnetically-induced-transparency ground-state cooling of long ion strings, *Phys. Rev. A* **93**, 053401 (2016).
- [32] C. Liu, Z. Dutton, C. H. Behroozi, and L. V. Hau, Observation of coherent optical information storage in an atomic medium using halted light pulses, *Nature (London)* **409**, 490 (2001).
- [33] P. Ranitovic, X. M. Tong, C. W. Hogle, X. Zhou, Y. Liu, N. Tushima, M. M. Murnane, and H. C. Kapteyn, Controlling The xuv Transparency of Helium Using Two-Pathway Quantum Interference, *Phys. Rev. Lett.* **106**, 193008 (2011).
- [34] A. Adler, A. Rachman, and E. J. Robinson, A time-dependent theory of resonant multiphoton ionization of atoms by short pulses. I. Weak-field results for the two-photon ionization of caesium, *J. Phys. B* **28**, 5057 (1995).
- [35] V. Rodríguez, Positronium ionization by short UV laser pulses: Splitting of the ATI peaks by Rabi oscillations, *Nucl. Instrum. Methods B* **247**, 105 (2006).
- [36] S. Pabst, D. Wang, and R. Santra, Driving Rabi oscillations at the giant dipole resonance in xenon, *Phys. Rev. A* **92**, 053424 (2015).
- [37] D. A. Tumakov, D. A. Telnov, G. Plunien, and V. M. Shabaev, Photoelectron spectra after multiphoton ionization of Li atoms in the one-photon Rabi-flopping regime, *Phys. Rev. A* **100**, 023407 (2019).
- [38] E. Saglamyurek, T. Hrushevskyi, A. Rastogi *et al.*, Coherent storage and manipulation of broadband photons via dynamically controlled Autler-Townes splitting, *Nat. Photon.* **12**, 774 (2018).
- [39] J. Kim, J. S. Lim, H.-R. Noh, and S. K. Kim, Experimental observation of the Autler-Townes splitting in polyatomic molecules, *J. Phys. Chem. Lett.* **11**, 6791 (2020).
- [40] P. L. Knight, AC stark splitting of photoelectron energy spectra in multiphoton ionisation, *J. Phys. B* **11**, L511 (1978).
- [41] M. G. Girju, K. Hristov, O. Kidun, and D. Bauer, Nonperturbative resonant strong field ionization of atomic hydrogen, *J. Phys. B* **40**, 4165 (2007).
- [42] M. G. Bustamante, V. D. Rodríguez, and R. O. Barrachina, Secondary peaks in the atomic ionization by a resonant laser pulse, *J. Phys.: Conf. Ser.* **397**, 012014 (2012).
- [43] Q. Liao, Y. Zhou, C. Huang, and P. Lu, Multiphoton Rabi oscillations of correlated electrons in strong-field nonsequential double ionization, *New J. Phys.* **14**, 013001 (2012).
- [44] Y. Chen, Y. Zhou, Y. Li, M. Li, P. Lan, and P. Lu, Rabi oscillation in few-photon double ionization through doubly excited states, *Phys. Rev. A* **97**, 013428 (2018).
- [45] B. Walker, M. Kaluža, B. Sheehy, P. Agostini, and L. F. DiMauro, Observation of Continuum-Continuum Autler-Townes Splitting, *Phys. Rev. Lett.* **75**, 633 (1995).
- [46] R. Grobe and J. H. Eberly, Observation of coherence transfer by electron-electron correlation, *Phys. Rev. A* **48**, 623 (1993).
- [47] J. H. Shirley, Solution of the Schrödinger equation with a Hamiltonian periodic in time, *Phys. Rev.* **138**, B979 (1965).
- [48] M. Wollenhaupt, A. Assion, O. Bazhan, C. Horn, D. Liese, C. Sarpe-Tudoran, M. Winter, and T. Baumert, Control of interferences in an Autler-Townes doublet: Symmetry of control parameters, *Phys. Rev. A* **68**, 015401 (2003).
- [49] M. Bagheri, U. Saalman, and J. M. Rost, Essential Conditions for Dynamic Interference, *Phys. Rev. Lett.* **118**, 143202 (2017).
- [50] W.-C. Jiang, S.-G. Chen, L.-Y. Peng, and J. Burgdörfer, Two-Electron Interference in Strong-Field Ionization of He by a Short Intense Extreme Ultraviolet Laser Pulse, *Phys. Rev. Lett.* **124**, 043203 (2020).
- [51] P. V. Demekhin and L. S. Cederbaum, Dynamic Interference of Photoelectrons Produced by High-Frequency Laser Pulses, *Phys. Rev. Lett.* **108**, 253001 (2012).
- [52] W.-C. Jiang and J. Burgdörfer, Dynamic interference as signature of atomic stabilization, *Opt. Express* **26**, 19921 (2018).
- [53] C. J. Joachain, N. J. Kylstra, and R. M. Potvliege, *Atoms in Intense Laser Fields* (Cambridge University Press, Cambridge, England, 2011).
- [54] M. Fleischhauer, A. Imamoglu, and J. P. Marangos, Electromagnetically induced transparency: Optics in coherent media, *Rev. Mod. Phys.* **77**, 633 (2005).
- [55] U. Fano, Effects of configuration interaction on intensities and phase shifts, *Phys. Rev.* **124**, 1866 (1961).